

Effect of Sintering Conditions on the Thermal Properties of Printable Metal Nanoparticle Ink Studied by Thermoreflectance

Md Saifur Rahman¹, Mizanur Rahman², Simone Pisana^{1,2}, Gerd Grau¹

¹ Department of Electrical Engineering and Computer Science
Lassonde School of Engineering, York University
4700 Keele Street
Toronto, ON, M3J 1P3
Canada

² Department of Physics and Astronomy
Faculty of Science, York University
4700 Keele Street
Toronto, ON, M3J 1P3
Canada

ABSTRACT

Metal nanoparticle inks are promising to fabricate conductors for low-cost, printed electronics. Low electrical resistivity can be achieved by nanoparticle sintering. The thermal properties of metal nanoparticle thin films have not been studied extensively but can yield great insights for the optimization of the sintering conditions. For example, in laser sintering, monitoring the changes in thermal conductivity over different stages of the process can help estimating the local temperature as well as the electrical conductivity of the film. In this work, we use frequency-domain thermoreflectance to measure these properties in a silver nanoparticle thin film thermally sintered *ex-situ*. The film is fabricated by spin coating a commercial printable silver ink with monodispersed 35 nm silver nanoparticles surrounded by a ligand. Using frequency-domain thermoreflectance (FDTR), we measured the thermal conductivity of the thin film by modulating the heat flux over a wide range of frequencies up to 50 MHz. An increase of thermal conductivity with increasing sintering temperature is observed up to a sintering temperature of 155°C, as measured by thermoreflectance or inferred through the Wiedemann-Franz Law based on electrical conductivity measurements. The results are corroborated with material characterization by Scanning Electron Microscopy (SEM) and Energy Dispersive Spectroscopy (EDS). The thermal and electrical properties are correlated throughout the different stages of sintering. For unsintered films, thermoreflectance gives more accurate values of thermal conductivity because it measures thermal conduction by both electrons and phonons. The Wiedemann-Franz Law underestimates the thermal conductivity by 50% in the unsintered case, which is problematic for modeling and optimization of the sintering process. In the sintered state, thermoreflectance and electrical conductivity measurements are in good agreement, as the contribution to heat transport is dominated by electrons. The thermoreflectance metrology can be used as a non-contact method to determine film conductivity, both thermal and electrical, during manufacturing processes involving nanoparticle inks.

Keywords— Printed Electronics, Silver Nanoparticles, Sintering, Thin films, Thermoreflectance, Thermal Conductivity, Electrical Conductivity, Solution Processing

1. INTRODUCTION

Printed electronics is a promising technology to fabricate electronics using conventional printing techniques. Devices and systems are made in an additive fashion with advantages including low cost, large area, and compatibility with flexible substrates such as plastic and paper^{1,2}. Many different microelectronic devices have been demonstrated using printing techniques including semiconductor devices such as transistors³, thermal devices such as heaters⁴, thermoelectric energy harvesters⁵ and temperature sensors⁶. In printed electronics, metal nanoparticle (MNP) solutions are one of the promising candidates for creating conductive patterns on low-cost substrates. High solute mass loading enables low resistance tracks⁷. After depositing the printed pattern on a substrate, the nanoparticles are sintered at an elevated temperature to transform the ink into a conductor. Compared to the bulk melting temperature of metals, the sintering temperature is significantly depressed by the small size and large surface area of the nanoparticles. The sintering process can be subdivided into three main steps. Firstly, the solvent is dried off. Secondly, the ligands that encapsulate particles in solution decompose. Thirdly, the nanoparticles fuse together. Inter-atomic diffusion, forced by the

tendency to minimize surface energy, leads to the grains growing and merging together to form a continuous percolating structure. This structure facilitates seamless transport of carriers, both electrons and phonons⁸.

The most important metric to quantify the quality of a sintered metal nanoparticle film is the electrical conductivity. Measuring electrical conductivity during process development and during manufacturing is critical. Traditional electrical measurements require dedicated contacts to be fabricated or probes that can scratch the material and take time to align. Here, we demonstrate that laser-based thermoreflectance measurements can be used to determine thermal conductivity, which is closely correlated with electrical conductivity for sintered films. This is a fast and contactless probing technique that can be used for process monitoring in a manufacturing setting. It measures conductivity more directly than simple reflectivity^{9,10}. Thermal conductivity is also an important property of printed nanoparticle films in its own right. Knowing the change of thermal conductivity as sintering progresses is important for modeling and optimizing the sintering conditions, especially for novel high-rate alternative sintering techniques such as laser¹¹ and intense pulsed light (IPL)¹² sintering. It is also critical to know thermal conductivity for applications where overheating can degrade device performance such as high-current circuits as well as for thermal devices. There have been reports of measuring the thermal conductivity of printed metal nanoparticle films^{13,14}. Electrical conductivity was measured and related to thermal conductivity via the Wiedemann-Franz Law. However, we show here that at the early stages of sintering, when the percolating network for electrons is not established yet, a significant fraction of the heat is transported by phonons. Therefore, the heat conductivity would be underestimated if one only considers the electronic contribution during sintering.

Thermoreflectance is a novel technique for measuring the thermal properties of thin films, especially thermal conductivity, that has generated much interest because of its applicability to many types of materials¹⁵. This method exploits the thermorefective property of materials, the relative change in the sample's surface reflectivity as a function of temperature. A modulated pump laser is used to heat up the surface of the sample, and a probe laser is impinged upon this locally heated area and its reflection is monitored. As the sample's temperature oscillates from the pump's heat flux and its reflectivity changes, there are changes in magnitude and phase of the reflected light. These changes are correlated to the thermal properties of the material via fitting with the solution of the thermal diffusion equation¹⁶. Typical thermoreflectance measurements rely on a metallic transducer deposited on the sample surface to absorb the pump light and to yield a thermoreflectance signal. However, the addition of this transducer layer complicates the sample preparation and lowers sensitivity to measurement of high diffusivity materials such as metal thin films. Here the silver MNPs are directly used as a transducer and material being tested; this is made possible by the silver having a sufficiently strong thermoreflectance coefficient at the probe wavelength and having no other layer in the sample that can absorb the pump light. To date, there are no reports on measuring the thermal properties of MNPs during sintering via thermoreflectance. Here, in this work, in-plane thermal conductivities of silver thin films sintered at different temperatures are measured with frequency-domain thermoreflectance (FDTR) and compared with results obtained using the Wiedemann-Franz Law.

2. EXPERIMENTAL

2.1 Fabrication

Nanoparticle films are fabricated on glass using a commercial silver nanoparticle ink (ANP DGP 40LT-15C). The particle diameter is 35nm and the major solvent is triethylene glycol monoethyl ether (TGME). To form a uniform thin film with thickness 80 ± 15 nm, spin coating is used with spin speed 2000 RPM for 60s.

The prepared films are subjected to a drying step at a temperature of 35°C before the sintering. The films are sintered on a hotplate at different temperatures ranging from 45°C to 185°C. Both the drying step and low temperature sintering (45°C) continues until the solvent is dried off. Usually, these steps take around 5-6 hours. The high temperature sintering (65-185°C) is carried out for 30 minutes.

2.2 Characterization

The details of the setup for thermal conductivity measurement with FDTR have been published elsewhere¹⁷. Figure 1 shows a schematic of our measurement setup. It is based on two continuous wave (CW) lasers operating at wavelengths of 515 nm (pump) and 785 nm (probe). The pump laser is modulated with an analog signal and the probe laser remains unmodulated. A 40X objective is used to focus the pump laser onto the sample. Optical isolators are used for both beams to prevent back reflections into the lasers. A polarizing beam splitter (PBS), together with a quarter wave plate (QWP), maximizes the amount of light reaching the detector. No transducer layer is used on top of the sample as the detected signal amplitude coming from the bare silver sample was strong enough to carry out the experiment. Due to the absorption of the modulated pump beam, the periodic heat flux causes the surface temperature to change periodically at the modulation frequency, but with an additional thermal phase θ_{thermal} . Two measurements are carried out to isolate this thermal phase from other experimental contributions to the phase signal, as is common in FDTR measurements. The first measurement, referred to as thermal measurement, is carried out measuring the probe beam ($\theta_1 = \theta_{\text{thermal}} + \theta_{\text{optical}} + \theta_{\text{electrical}} + \theta_{\text{reference}}$). The second measurement is a reference measurement measuring just the pump beam ($\theta_2 = \theta_{\text{optical}} + \theta_{\text{electrical}} + \theta_{\text{reference}}$). As both beams travel the same distance electrically and optically, $\theta_{\text{thermal}} = \theta_1 - \theta_2$. To prevent laser sintering by the pump beam and altering the properties of the nanoparticle film, the laser power is kept small (~100 μ W); selected such that the DC temperature rise at the surface is limited to 30°C. The measured thermal phase is fit to a model based on the Fourier Law to obtain the thermal conductivity of the thin film¹⁷.

Four-point probe is used to measure electrical sheet resistance (Keithley SMU 2450 Source Meter with SP4 Four Point Head). The sheet resistance is then converted to resistivity with the film thickness measured with an optical profilometer (Contour GT, Bruker) using the following equation (1). Here, R_s and t are the sheet resistance and film thickness.

$$\rho = R_s * t \quad (1)$$

$$k = \sigma * L * T = \frac{L * T}{\rho} \quad (2)$$

Electrical conductivity is correlated with thermal conductivity using the Wiedemann-Franz Law, equation (2), where k is thermal conductivity, σ is electrical conductivity from sheet resistance, T is room temperature and L is the Lorentz number which is $2.37 * 10^{-8} \text{ W}\Omega/\text{K}^2$ for silver.

A Field Emission Gun Scanning Electron Microscope (FEGSEM, Fisher Quanta 3D) is used for capturing images in the nanometer range and studying the surface morphology of the films at different stages of the sintering process. The same equipment is used to examine the elemental composition of the films by Energy Dispersive Spectroscopy (EDS). Single point as well as a large area, for both sintered and unsintered films, are analyzed.

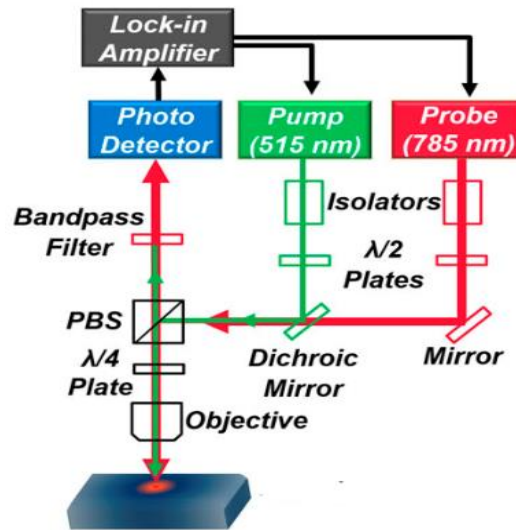


Figure 1. FDTR setup; a pump laser periodically heats up a spot whereas a probe laser is reflected from this spot with an additional thermal phase. The mirrors and objective are used to guide and focus the beams. A bandpass filter and photo detector are used to collect the reflected probe signal and convert it to an electrical signal.

3. RESULTS AND DISCUSSION

The electrical conductivity increases as the sintering temperature increases from room temperature. Figure 2(a) shows the change. From 35 to 145°C it monotonically increases from $7.36 * 10^5 \text{ S/m}$ to $1.869 * 10^7 \text{ S/m}$. The sheet resistance exhibits the opposite trend, declining from $16.56 \Omega/\text{sq}$ to $0.87 \Omega/\text{sq}$. After 145°C, the increase in electrical conductivity is very limited, remaining close to the value of 145°C. At 185°C there is decline in electrical conductivity. The highest electrical conductivity was found to be $2.235 * 10^7 \text{ S/m}$ for films sintered at 175°C, which is 35.5% of the electrical conductivity of bulk silver.

Figure 2(b) shows the thermal phase vs frequency plot for a film sintered at 85°C. This is a typical example to show, in general, how well the diffusive thermal model¹⁶ fits the measured data. Figure 2(c) shows in-plane thermal conductivity from FDTR measurements and thermal conductivity calculated from electrical conductivity using the Wiedemann-Franz Law with respect to different sintering temperatures. For both measurements, thermal conductivity saturates with sintering temperature. The slope of conductivity with temperature is initially modest up to 125°C sintering. A jump of 48W/m.K is observed when the sintering temperature is increased from 125°C to 145°C. This is the temperature window when grains start to grow larger via neck formation as discussed later with the aid of SEM images. After 145°C, any increment of sintering temperature does not affect the thermal conductivity greatly. Both FDTR and thermal conductivity from electrical conductivity follow the same trend as sintering temperature increases, although a gap of 5.6-13 W/m.K. is always present between them. This occurs because the FDTR measurement is a direct thermal measurement, which includes both phononic and electronic heat transport. In contrast, the Wiedemann-Franz Law only accounts for the electronic contribution. Figure 2(d) shows the change of the phononic contribution of heat transport with sintering temperature increment. In the case of films sintered at low temperatures (35°C to 105°C), that gap i.e. the phononic contribution is around 5.6-10.61 W/m.K, whereas, this increases to 12-13 W/m.K for films sintered at high temperatures (125°C to 185°C). It is expected that the phononic contribution would increase as sintering progresses. Larger grain size and correspondingly larger mean free path before phonons scatter at grain boundaries result in a larger phononic contribution to thermal conductivity. To explain this behavior in detail, we investigated the surface morphology using SEM. Overall, the

phononic contribution as a fraction of overall thermal conductivity decreases with increasing sintering temperature as the electronic contribution increases. This means at high sintering temperatures thermal conductivity can be used to predict electrical conductivity and FDTR can be used to determine the sintering state of nanoparticle films.

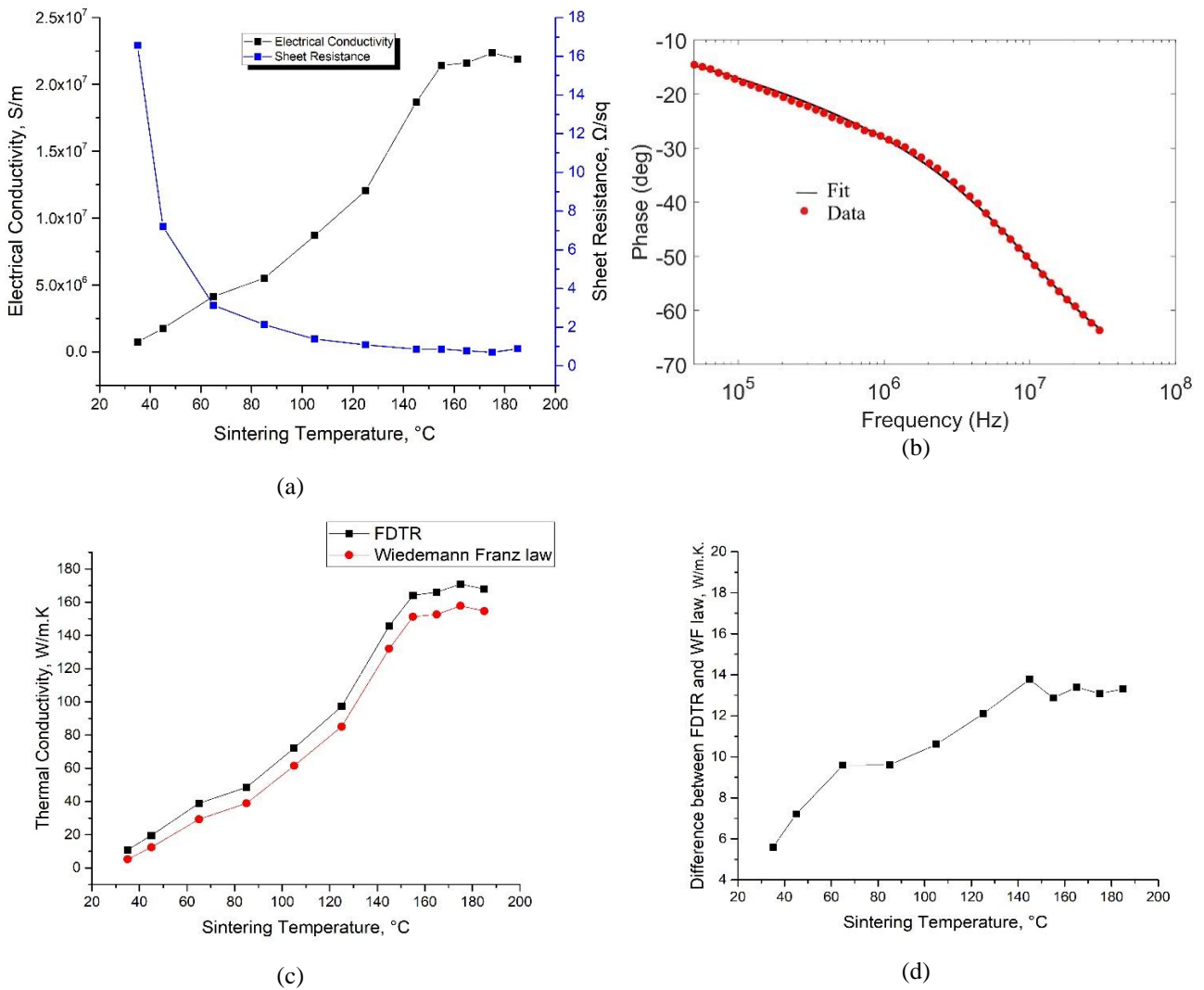


Figure 2. (a) Change of the electrical conductivity and sheet resistance as a function of sintering temperature. Films become more conductive with increasing sintering temperature. (b) Representative example of measured thermal phase. Solid line represents fit using diffusive thermal model illustrating good agreement between fit and measured data. (c) Thermal conductivity after sintering at different temperatures measured using FDTR and calculated from electrical conductivity using Wiedemann-Franz Law. (d) Difference between two measurements i.e. phononic contribution to heat transport vs increment of sintering temperature. The phononic contribution increases with sintering temperature.

Figure 3 shows SEM images of the film surface for different sintering temperatures. Up to 85°C , there is no visible change in the size of the grains. Conductivity still rises with sintering temperature because the efficacy of the ligands encapsulating the nanoparticles decreases. Ligand disassociation and transformation to amorphous carbon starts to happen which exposes the nanoparticles to their neighboring nanoparticles. The extent of this contact increases with sintering temperature as has been observed before¹⁸. At 105°C , the onset of neck formation occurs, necks form between some nanoparticles. At this temperature, the phononic contribution starts to increase because of decreased scattering. During the next stage, at 125°C , the grain shape is not spherical anymore, they assume an elongated form. Beyond 145°C , individual grains are hardly visible in SEM. Nanoparticles have coalesced together and formed larger grains. The number of pores increases due to smaller grains merging together because of Ostwald Ripening¹⁹. The formation of a semi-continuous film with no visible grains explains the jump of thermal conductivity from 125°C to 145°C . After 145°C , the film morphology remains the same, so did the measured values of thermal conductivity. However, at 185°C , the number of pores and their size further increases due to excessive sintering. This

affects both thermal and electrical conductivity measurements, which decline slightly. It can be concluded that a safe temperature range for fully sintering this ink is from 155°C to 175°C. The best thermal conductivity of 170.9 W/m.K. is found at 175°C, 40% of the thermal conductivity of bulk silver.

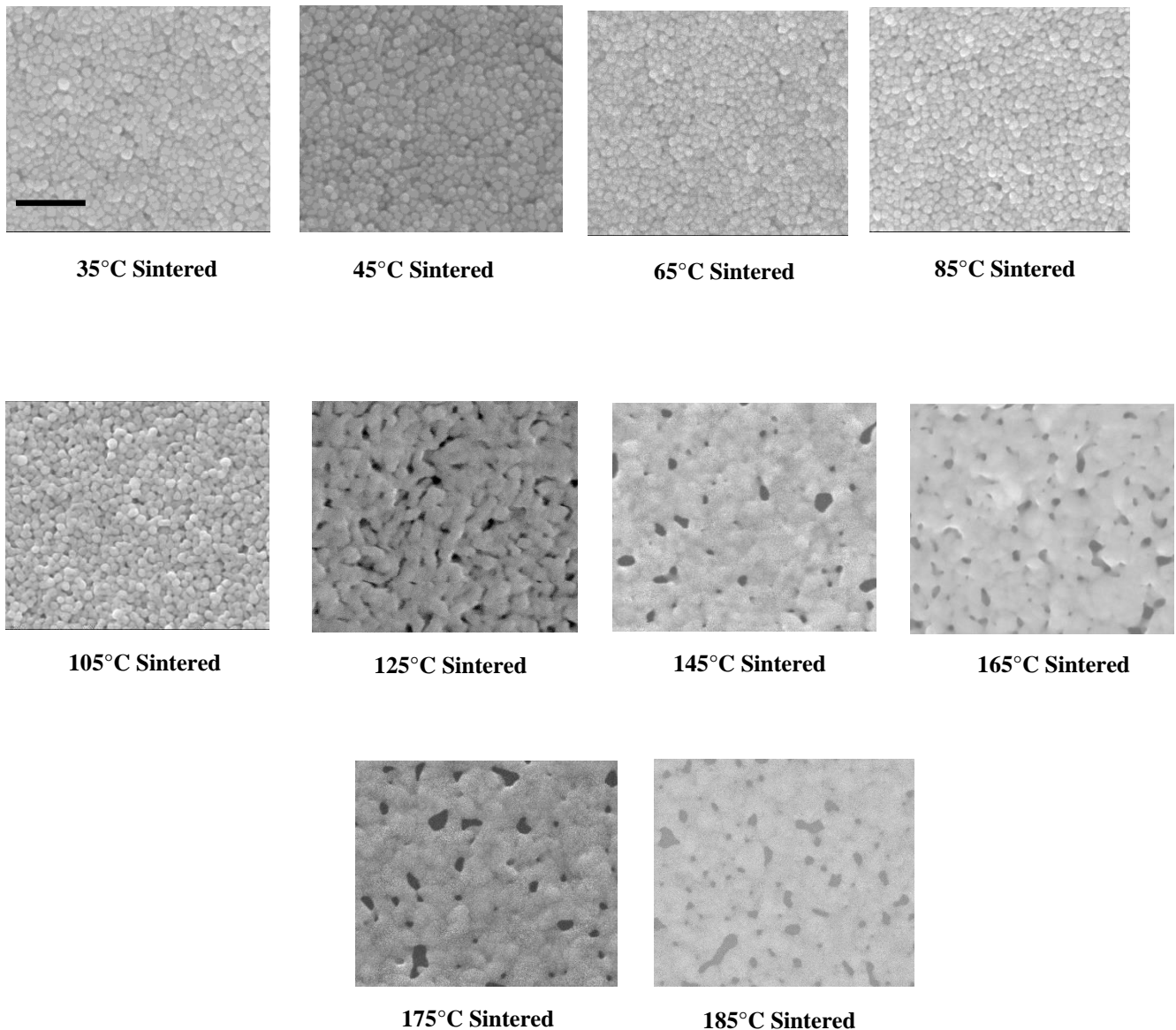


Figure 3. SEM images of films sintered at different temperatures. One can clearly observe unsintered individual nanoparticles for films treated at low temperatures up to 85°C. Above this temperature, nanoparticles merge together, and grains grow. Eventually, excessive grain growth leads to voids in the film, which is very visible at 185°C. The scale bar represents 500 nm.

Energy Dispersive Spectroscopy (EDS) reveals the fraction of different elements present in spot radius of a few microns as well as a 1mm X 1mm area of the sample. The unsintered film contains carbon and silver. Contributions from the underlying glass substrate such as sodium, magnesium, silicon, potassium, calcium and oxygen are ignored. After sintering, the carbon content is reduced to zero. This signifies that the carbon containing ligand chains are mostly removed by sintering at 165°C. When a large area (1mm X 1mm) is measured by elemental analysis, a trace amount of carbon is still found. This means even at a high sintering temperature the ligands are not fully removed, which has been observed before ¹⁸.

4. CONCLUSION

The thermal conductivity of solution-processed silver nanoparticle films is measured using frequency-domain thermoreflectance without the need for additional steps such as deposition of a transducer layer. We demonstrate that FDTR measurements can be used to determine the sintering state of nanoparticle films. FDTR results are correlated with electrical conductivity measurements. Films sintered at high temperature exhibit good agreement between the two methods. Therefore,

FDTR can be used as a non-contact measurement technique to monitor conductivity in printed electronics manufacturing. Unsintered films exhibit poor agreement between thermal conductivity measured directly using FDTR and indirectly from electrical conductivity using the Wiedemann-Franz Law. The Wiedemann-Franz Law underestimates thermal conductivity because phonons contribute significantly to thermal conductivity in the unsintered state. Thermal conductivity measured using FDTR can therefore improve modeling accuracy and optimization of the sintering process.

5. ACKNOWLEDGMENTS

We acknowledge the support of the Natural Sciences and Engineering Research Council of Canada (NSERC), funding reference number STPGP 521480-18.

6. REFERENCES

1. Arias AC, MacKenzie JD, McCulloch I, Rivnay J, Salleo A. Materials and Applications for Large Area Electronics: Solution-Based Approaches. *Chem Rev.* 2010. doi:10.1021/cr900150b
2. Grau G, Kitsomboonloha R, Swisher SL, Kang H, Subramanian V. Printed transistors on paper: Towards smart consumer product packaging. *Adv Funct Mater.* 2014. doi:10.1002/adfm.201400129
3. Kang B, Lee WH, Cho K. Recent advances in organic transistor printing processes. *ACS Appl Mater Interfaces.* 2013. doi:10.1021/am302796z
4. Zeng P, Tian B, Tian Q, et al. Screen-Printed, Low-Cost, and Patterned Flexible Heater Based on Ag Fractal Dendrites for Human Wearable Application. *Adv Mater Technol.* 2019. doi:10.1002/admt.201800453
5. Varghese T, Hollar C, Richardson J, et al. High-performance and flexible thermoelectric films by screen printing solution-processed nanoplate crystals. *Sci Rep.* 2016;6(1):33135. doi:10.1038/srep33135
6. Aliane A, Fischer V, Galliari M, et al. Enhanced printed temperature sensors on flexible substrate. *Microelectronics J.* 2014. doi:10.1016/j.mejo.2014.08.011
7. Puchalski M. The Applicability of Global and Surface Sensitive Techniques to Characterization of Silver Nanoparticles for Ink-Jet Printing Technology. In: Kowalczyk PJ, ed. Rijeka: IntechOpen; 2010:Ch. 3. doi:10.5772/8507
8. Huang D, Liao F, Molesa S, Redinger D, Subramanian V. Plastic-Compatible Low Resistance Printable Gold Nanoparticle Conductors for Flexible Electronics. *J Electrochem Soc.* 2003;150(7):G412. doi:10.1149/1.1582466
9. Zenou M, Ermak O, Saar A, Kotler Z. Laser sintering of copper nanoparticles. *J Phys D Appl Phys.* 2014;47(2):025501. doi:10.1088/0022-3727/47/2/025501
10. Lee DG, Kim DK, Moon YJ, Moon SJ. Effect of temperature on electrical conductance of inkjet-printed silver nanoparticle ink during continuous wave laser sintering. *Thin Solid Films.* 2013;546:443-447. doi:10.1016/j.tsf.2013.05.103
11. Yoon YH, Yi S-M, Yim J-R, Lee J-H, Rozgonyi G, Joo Y-C. Microstructure and electrical properties of high power laser thermal annealing on inkjet-printed Ag films. *Microelectron Eng.* 2010;87(11):2230-2233. doi:10.1016/J.MEE.2010.02.008
12. Abbel R, van Lammeren T, Hendriks R, et al. Photonic flash sintering of silver nanoparticle inks: a fast and convenient method for the preparation of highly conductive structures on foil. *MRS Commun.* 2012;2(4):145-150. doi:10.1557/mrc.2012.28
13. Choi JH, Ryu K, Park K, Moon SJ. Thermal conductivity estimation of inkjet-printed silver nanoparticle ink during continuous wave laser sintering. *Int J Heat Mass Transf.* 2015;85:904-909. doi:10.1016/j.ijheatmasstransfer.2015.01.056
14. Lee DG, Kim DK, Moon YJ, Moon S-J. Estimation of the Properties of Silver Nanoparticle Ink During Laser Sintering via I^2R In-Situ I^2R Electrical Resistance Measurement. *J Nanosci Nanotechnol.* 2013;13(9):5982-5987. doi:10.1166/jnn.2013.7650
15. Schmidt AJ, Cheaito R, Chiesa M. A frequency-domain thermoreflectance method for the characterization of thermal properties. *Rev Sci Instrum.* 2009;80(9). doi:10.1063/1.3212673
16. Feser JP, Cahill DG. Probing anisotropic heat transport using time-domain thermoreflectance with offset laser spots. In: *Review of Scientific Instruments.* ; 2012. doi:10.1063/1.4757863
17. Rahman M, Shahzadeh M, Braeuninger-Weimer P, Hofmann S, Hellwig O, Pisana S. Measuring the thermal properties of anisotropic materials using beam-offset frequency domain thermoreflectance. *J Appl Phys.* 2018;123(24). doi:10.1063/1.5033966
18. Volkman SK, Yin S, Bakhishev T, Puntambekar K, Subramanian V, Toney MF. Mechanistic Studies on Sintering of Silver Nanoparticles - Chemistry of Materials (ACS Publications). 2011. <http://pubs.acs.org/doi/full/10.1021/cm202561u>.
19. Alemán J V., Chadwick A V., He J, et al. Definitions of terms relating to the structure and processing of sols, gels, networks, and inorganic-organic hybrid materials (IUPAC Recommendations 2007). *Pure Appl Chem.* 2007;79(10):1801-1829. doi:10.1351/pac200779101801